Cell Reports
Physical Science

CellPress
OPEN ACCESS

Article

Mycelium-based wood composites for light weight and high strength by experiment and machine learning

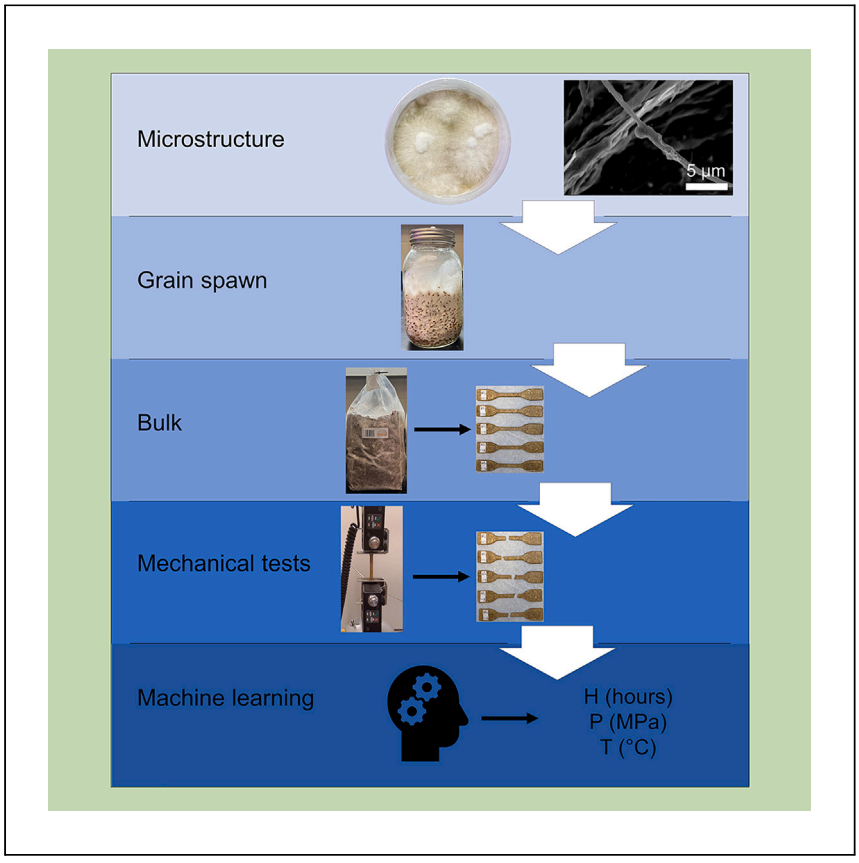

Yang et al. study the mechanics of mycelium-wood-fiber-based composites and reveal how their material functions, including density, Young's modulus, ultimate strength, and toughness modulus, vary with the processing conditions. This mycelium-based composite has higher mechanical strength than samples without mycelium and is more energy efficient in preparation.

Libin Yang, Zhao Qin

zqin02@syr.edu

Highlights

Mycelium grows on stalk fibers and helps to form composites without adhesive

Heat press helps to integrate mycelium and substrate to form composites

Mycelium composite has an ultimate strength and Young's modulus close to a fiberboard

Machine learning based on the experiments helps to optimize treatment conditions

Yang & Qin, Cell Reports Physical Science 4, 101424
June 21, 2023
https://doi.org/10.1016/j.xcrp.2023.101424

Cell Reports
Physical Science

CellPress
OPEN ACCESS

Article

Mycelium-based wood composites for light weight and high strength by experiment and machine learning

Libin Yang[1,2] and Zhao Qin[1,2,3,4,*]

SUMMARY

Wood composites composed of recombined wood fibers heavily depend on synthetic adhesives for mechanical strength. Here, we focus on using mycelium to gain wood composites and integrating experiments and machine learning for better mechanical properties. We grow mycelium *Pleurotus eryngii* on stalk fibers as a natural adhesive by forming a secondary fibrous network. We find that mycelium enhances the composite mechanics but breaks down at high temperatures. We obtain composite samples with an ultimate strength of up to 12.99 MPa with a Young's modulus of 3.66 GPa, which is higher than samples without mycelium obtained from the same condition. We build machine learning models based on experimental tests to predict the material functions for any treatment conditions. The composite with mycelium requires a relatively lower temperature, higher pressure, and shorter pressing time to yield higher strength and modulus. Our results could be useful for engineering composites from living materials.

INTRODUCTION

Wood composites are an ever-evolving product sector increasingly used in various engineering applications, and their demand has been on an upward trend for decades.[1] Wood composite is a broad term that encompasses a vast array of composites composed of wood sheets, fibers, and particles integrated via different adhesives (e.g., medium-density fiberboard [MDF] and particle board, plywood, oriented strand board, and wood polymer composites).[2–6] They are often used as a substitute for natural wood for non-structural applications (e.g., fencing, decking, furniture, temporary construction, floorings, windows, and doors).[7] The new generation of the wood composite can be multifunctional by incorporating fibers from different wood species with engineering fibers (e.g., glass, carbon, plastic) and adhesive resins.[8–11] Functions beyond the natural wood can be realized during the manufacturing process by design (e.g., any thicknesses, grades, size, and exposure durability to UV, high temperature, etc.).[12,13] Wood fibers are the main component that contribute to the low cost of the composite material because most of them are conventionally treated as wastes, fuels, or landfills (e.g., cotton, flax, or hemp from crops, Christmas trees, landscaping, wastepaper, and agriculture byproducts or regenerated cellulose fiber[14]). These wood fibers lack intermolecular interactions that bind them to form a bulk material as hemicellulose and lignin do in natural wood.[15] Thus, the production of wood composites depends on the source and physical properties of these foreign adhesives that are added during manufacturing, which in turn affect the material functions (e.g., mechanical, thermal, chemical) and environmental impact (e.g., embodied carbon) of the composites.[1,16–18]

[1]Laboratory for Multiscale Material Modelling, Syracuse University, 151L Link Hall, Syracuse University, Syracuse, NY 13244, USA

[2]Department of Civil and Environmental Engineering, Syracuse University, 151L Link Hall, Syracuse University, Syracuse, NY 13244, USA

[3]The BioInspired Institute, Syracuse University, NY 13244, USA

[4]Lead contact

*Correspondence: zqin02@syr.edu

https://doi.org/10.1016/j.xcrp.2023.101424

Synthetic wood adhesives are widely used in the wood composites industry. Still, they have disadvantages, including durability to humidity and aging in time, causing warping to wood structures, as well as long-term environmental effects, including carbon emission during material synthesis; the slow release of formaldehyde, which is hazardous to human health[19–21]; and a higher fire hazard than solid wood.[12,22] Moreover, these synthetic adhesives are derived from non-renewable sources (e.g., petroleum and natural gas)[23,24] that are limited by their storage. There is a growing interest in developing eco-friendly wood adhesives (e.g., lignin-, starch-, and protein-based adhesives) derived from renewable sources.[18,25] They have a high molecular weight and are fully biocompatible and biodegradable.[26] Lignin is a suitable wood adhesive for its phenolic structures[25] and forms hydrogen bonds to cellulose and other desirable material features, including high hydrophobicity, a low glass transition temperature, and low polydispersity.[27–29] Its adhesion strongly depends on the molecular structure and, thus, the mechanics of the adhesive.[30] Starch is another natural adhesive that is available in most plants. It is cheap, easy to process, and forms an excellent thin film with strong adhesion. It was used for plywood manufacturing years ago.[31,32] However, starch-based composites have poor water resistance and a slow drying rate.[25] Protein-based adhesives have high viscosity, short pot life, and high sensitivity to water, and their material functions are sensitive to the sequence. Although it is possible to predict the protein structure from its sequence with machine learning algorithms,[33] its adhesion function at a large scale is still far from the molecular structure, making it elusive what key protein sequences are optimized for wood adhesion.[25,34,35]

Mycelium, another adhesive for wood composites, has attracted broad industrial interest in recent years.[36–40] Mycelium is the vegetative part of a fast-growing, regenerable fungus, consisting of a network of fine white filaments of 1–30 μm diameter.[41] It grows in the form of numerous branching fibers, attaching itself to the medium in which it grows.[42] The medium can be agricultural waste or any other material capable of providing nutrients for growth, such as wood, straws, husks, chaws, and bagasse of the mycelium.[43–45] The mycelium multiplies and produces numerous self-assembled bonds in the form of tiny fibers called hyphae, which cover the entire loose substrate and digest the substrate during its growth, binding it into a strong and natural composite.[46–48] Mycelium-based biocomposites have similar strength to expanded polystyrene (EPS) and are biodegradable.[49,50] Various properties of mycelium-based composites make it useful for different applications such as thermal and acoustic insulation.[51–53]

Here, we explore an efficient way to produce a mycelium-based wood composite with outstanding mechanical properties. Figure 1 shows the general structure of mycelium from microstructure to macroscale. Our results of the tensile test show that the mycelium-based sample has a higher ultimate strength. Moreover, our machine learning model provides a more reliable range of treatment conditions that can guide the wood composite synthesis for a specific mechanical function. Our study sheds light on developing new wood composites made of mycelium instead of polymer adhesives, leading to environmentally friendly materials for wide engineering applications.

RESULTS AND DISCUSSION

Wood composite samples from different substrates

To investigate how mycelium can be used as a general adhesive for different wood-based substrates, we prepared three other substrate materials to make mechanical

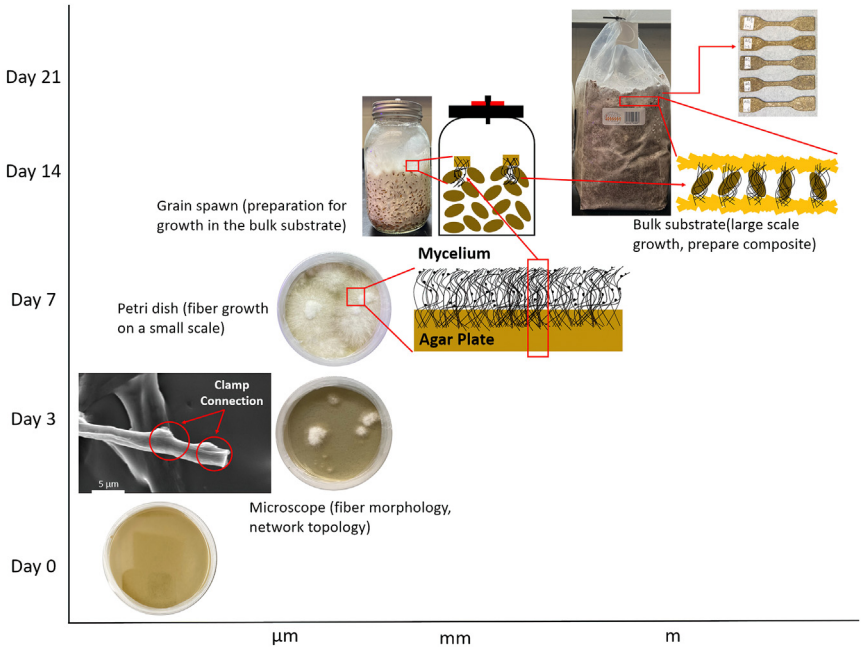

Figure 1. Multiscale structure of the mycelium in our study

From the bottom left, the figure shows the scanning electron microscopy (SEM) image of the mycelium network and mycelium's unique structure (i.e., thin straight fiber with clamp connection), as well as the two figures of the wet mycelium sample's growth on days 3 and 7 in the culturing disk. The schematics show the general process of preparation, including growth of mycelium in the Petri dish and jars, moving the incubated mycelium on the rye from the jar to the larger substrate, and heat pressing for samples for mechanical tests.

samples. We use *Pleurotus eryngii*, known as the king oyster, not only because spores grow in the mycelium, are easy to grow, and have high yield, but also because it is the same genus as the *Pleurotus ostreatus*.[41,54] The *P. ostreatus* is the most common species used in the experiment.[55] Ensuring the success of an experiment can be achieved by using fungi belonging to the same genus. The number of known fungal species alone exceeds 150,000, and scientists estimate that several million additional species could be yet to be discovered.[56] This vast diversity of fungi highlights the need for a systematic approach to experimental design, with careful consideration given to the selection of appropriate fungal strains. Choosing other species from the *Pleurotus* genus can avoid performing the same experiment with other researchers. Moreover, *P. eryngii* has been used to develop fungus-based aerogels for green thermal insulation materials, thermal management materials for electrical devices, durable acoustic materials, pollution adsorption materials, etc.[57] Therefore, *P. eryngii* is a suitable undeveloped species that can be applied to our experiments. The stalk (S) and S with mycelium (SM) are prepared by us. For comparison, we use the commercial mushroom grow kit,[58] a mixture of wheat bran, hardwood saw dust (fruit wood), spent coffee grounds, and other agriculture wastes for growing substrate and *P. eryngii* mycelium (HCM [hardwood mixed with coffee grounds and mycelium])

We use these three different raw materials and convert them into mechanical samples for testing. Figure 2A summarizes the key steps: we mix each of the raw materials (i.e., S, SM, HCM) with water by using a blender until the material becomes uniform sludge, transferring the sludge to a dog bone sample mold, and turning the sludge to solid dog bone samples with a 10-ton heat-press machine. We vary

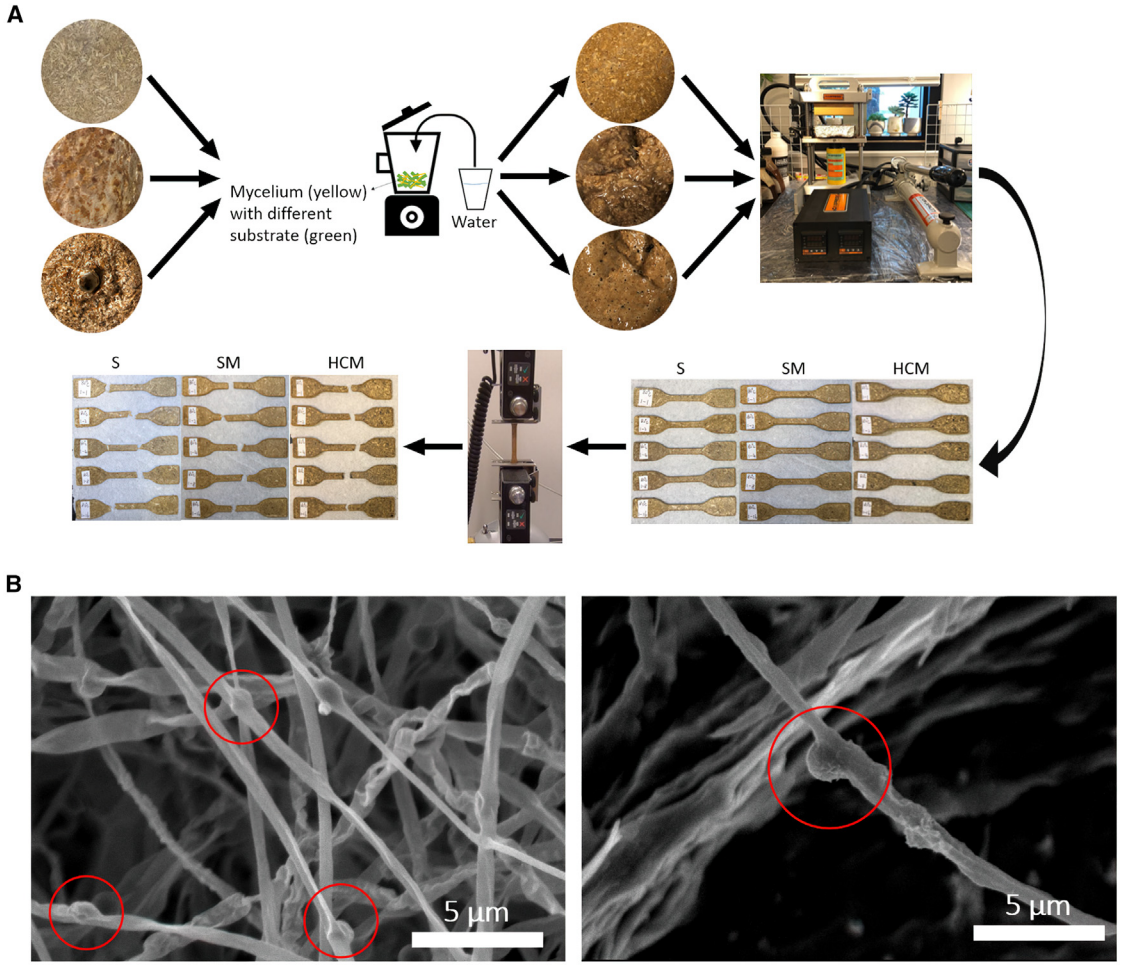

Figure 2. Processing of mycelium-based wood composites and their microstructural features

(A) The general process of the experiment. The dog bone samples shown in the figure are made with three different materials based on the 80°C and 6.75 MPa pressure combined with five different baking times, which are 1, 2, 4, 8, and 16 h (material → mix with water → mushy material → heat-press machine → test samples → Instron machine → broken samples).

(B) The SEM image of mycelium-based biocomposite material at room temperature dried for a month (left) and after the heat pressing of 90°C, baking time 16 h, and 20.27 MPa pressure (right).

the processing temperatures (i.e., 80°C, 90°C, and 100°C), pressures (i.e., 6.7, 14.3, and 20.3 MPa), and baking times (1, 2, 4, 8, and 16 h) for producing the samples. We have 135 samples, with 45 samples for each raw material for mechanical tests, as illustrated by Figure 2A. With this processing method, we obtain solid wood composite samples with densities varying from 0.8587 to 1.55 g/cm^3. It is noted that although the control group (S) lacks mycelium, the starch in the grains can still bind the S fibers together to form the solid material.

We compare the microscopic image of the mycelium sample in free air drying (~30 days) and heat-pressing conditions. All mycelium fibers become flat strips, and the clamp connection is buckled by losing its rounded shape in air drying. In contrast, the mycelium fibers are still cylindrical with the smoothly rounded clamp connection at the middle after heat press (i.e., SM, 90°C, 20.27 MPa, 16 h), as shown in Figure 2B. The flat fiber and the buckled clamp connection suggest that each mycelium fiber is a hollow tube filled with water with its cross-section profile supported by

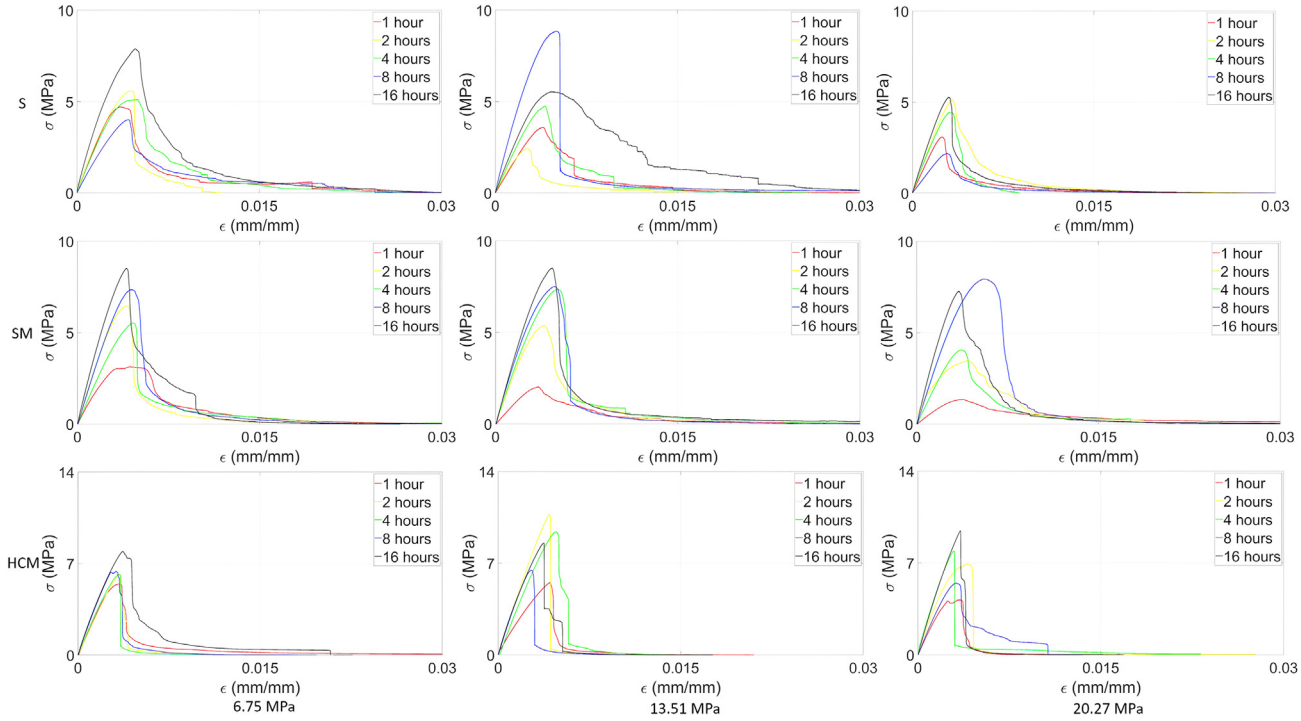

Figure 3. The stress-strain curve for dog bone samples tests the composites made of the pure stalk, stalk with mycelium, and hardwood mixed with coffee grounds and mycelium grown in it

Tests are based on samples prepared under 90°C with different pressures (6.75, 13.51, and 20.27 MPa) and baking times (1, 2, 4, 8, and 16 h).

internal moisture. Losing the water leads to a mechanically buckled shape. The intact mycelium shape of the heat-press sample suggests that the tens of hours of baking at 90°C is insufficient to empty the water within the mycelium fiber fully; therefore, its profile is intact even under much higher pressure than the atmosphere.

Mechanics of mycelium-based composites

We measure the bulk density and perform the tensile test on each sample with an Instron machine to understand the effects of mycelium and treatment conditions on the mechanical properties of the composite materials. Figure 3 summarizes the stress-strain curves of the mechanical samples made of the three different raw materials, different pressures, and baking times under 90°C (other loading curves for baking under 80°C and 100°C are summarized in Figure S2). It is shown that all the mechanical samples reach the ultimate tensile strength (σ_U), as the maximum stress, before the 1% strain, followed by a tail that accounts for energy dissipation during the failure. For SM samples, it is shown that most of the σ_U increases with a baking time of up to 8 h as more water is evaporated, leading to a more compact solid material in pressing. On the other hand, a baking time longer than 8 h yields weaker samples, as the long heat press can break the mycelium fiber into small pieces, as shown by microscopic images (Figure S2).

We found that the different substrates can significantly affect the ultimate strength. We measure the density of each sample (ρ) and compute Young's modulus (E), σ_U, and modulus of toughness (U_T) (see experimental procedures) for each of the samples (raw data for all the samples in Tables S1–S3). Table 1 summarizes all physical properties of the samples of maximum σ_U given by different raw materials. It is shown that σ_U = 9.70 MPa provided by SM is significantly larger than σ_U = 8.85 MPa given

Table 1. The maximum ultimate strength and other physical properties of a sample made of each raw material

Material properties	S	SM	HCM
σ_U (MPa)	8.85	9.70	12.99
E (MPa)	2669.5	2841.4	3664.8
U_T (MJ/m^3)	0.038	0.044	0.030
ρ (g/cm^3)	1.39	1.41	1.26

by S without mycelium, suggesting that σ_U increases by 10% when the density is increased by 1.6% by adding mycelium. Furthermore, the SM sample of the highest σ_U shows an advantage over the S sample of the highest σ_U by having a higher E by 6% and a higher U_T by 16%, suggesting that the mycelium can also significantly increase the material stiffness and toughness. Moreover, the highest σ_U = 12.99 MPa for all samples is obtained from HCM, which is 19% higher than the 10.89 MPa strength of a corn-straw-based biocomposite in literature.[59] It is noted that the material density for the highest σ_U is much less than the highest ρ value (1.53 g/cm^3 for SM and 1.54 g/cm^3 for HCM; Table S2 and S3), indicating that the composite strength does not monotonically increase with the material density, making it different from ideal cellular materials (e.g., porous PS).[60] We also consider all 45 other processing conditions and compute the difference in ρ, σ_U, E, and U_T for samples made of S, SM, and HCM. It is shown that by using the same processing conditions, ρ values of the samples made of SM and HCM increase by 11% compared with the samples made of S on average, while σ_U increases by 35% and 96%, E increases by 14% and 76%, and U_T increases by 47% and 7% for SM and HCM, respectively.

The results suggest that the mechanical advantage (σ_U, E, and U_T) of adding mycelium to wood composite is not limited to a specific processing condition but generally exists. These advantages in strength and modulus are very different from what is given by the scaling law of ideal cellular materials, as $\frac{\sigma_{U1}}{\sigma_{U2}} = \left(\frac{\rho_1}{\rho_2}\right)^{1.5}$ and $\frac{E_1}{E_2} = \left(\frac{\rho_1}{\rho_2}\right)^2$,[60] suggesting that adding the mycelium changes the interactions between the building blocks within the wood composite. We believe that HCM gives the highest strength mainly because of the higher content of mycelium, as the mycelium had already grown to fully occupy the substrate before our tests. In contrast, the total time for mycelium growth in SM is limited (14 days) in our lab. It is also noted that compared with the significant increment in σ_U and E, HCM does not give a much different U_T from S, indicating a negative effect on material toughness by having too much mycelium in the substrate. The unnecessary mycelium will reduce the flexibility of the composite and lead to brittle failure, which is shown again for different processing temperatures (80°C and 100°C) in Figure S3 in the Supplementary Information, as HCM reaches σ_U at a lower strain level without ductile tail after σ_U and agree with the recent observation that a flexible mycelium composite has a higher toughness than the brittle one.[61]

Design toward the specific mechanics of mycelium-based composites

We compute the specific mechanical properties σ_U/ρ, E/ρ, and U_T/ρ based on values summarized in Tables S1–S3, which account for the effective materials usage toward different mechanical functions, as shown by the Ashby plots in Figure 4. It is shown that the specific strength and modulus (Figure 4A) are highly correlated, which largely agrees with the Ashby plot of the other cellular materials (e.g., foams, cork, bone, wood),[62] suggesting that even though we have applied a heat-press treatment, the samples are largely similar to cellular materials, as both σ_U and E monotonically increases with ρ, and thus show overall agreement with the scaling

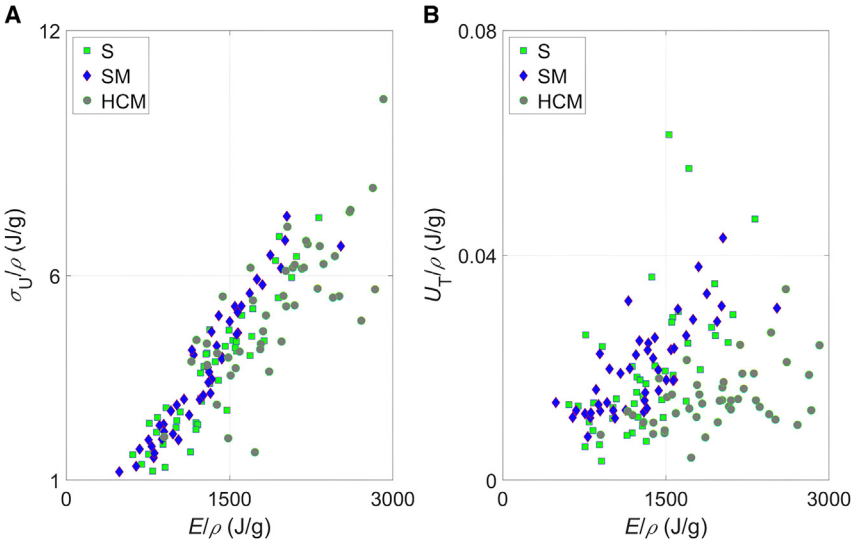

Figure 4. Ashby plots for specific mechanical properties of different wood composites

(A) Specific ultimate strength and Young's modulus normalized by density, showing that these two mechanical properties of the wood composite are well aligned, which largely agrees with the other cellular materials (e.g., foams, cork, bone, wood).[62]

(B) Specific modulus of toughness and Young's modulus normalized by density, showing that the toughness of the composites are highly dispersed and weakly determined by the Young's modulus.

laws of other cellular materials. However, neither U_T/ρ nor U_T shows a strong correlation with E/ρ or ρ of the composites, as shown in Figure 4B, indicating that their optimization is more complex than σ_U and E.

Table 2 summarizes the maximum specific mechanical properties with their corresponding processing conditions, which can help guide the treatment conditions for a specific optimized function. The temperature for yielding the best specific mechanical properties is likely from 90°C to 100°C, which agrees with the water evaporation temperature, reducing the water volume and making the wood fibers more compact for a higher density. However, there is no other universal treatment condition that can lead to all the maximum mechanical properties. It is shown that HCM gives the highest $\frac{\sigma_U}{\rho}$ = 10.32 and $\frac{E}{\rho}$ = 2,912.3 J/g with 4 h of baking time, which are much shorter than S and SM, suggesting that more mycelium in the raw material enables a higher specific strength and modulus as well as reduces the amount of baking time before reaching the optimal specific strength and modulus. Our samples have a similar $\frac{\sigma_U}{\rho}$ compared with the corn-straw-based biocomposite in literature,[59] while the $\frac{E}{\rho}$ of our samples is much larger (1,800 J/g) than that of the literature value,[59] suggesting that our samples are much stiffer with the same density. It is noted that the U_T/ρ values for all the S samples are smaller (0.085 J/g) than that of the literature value,[59] and adding the mycelium (SM and HCM) further reduces the specific toughness value. This result agrees with the fact that adding mycelium reduces the flexibility of the composite, leading to higher modulus but lower toughness, because a strong interaction by mycelium prevents the wood fibers from sliding, which accounts for a portion of energy dissipation of a fibrous material.[63,64]

Supervised machine learning for predicting the specific mechanics of mycelium-based composites

We utilized all experimental data by taking the processing conditions (i.e., time [h], pressure [P], temperature [T], material type [i.e., S, SM, and HCM]) as input

Table 2. The treatment conditions (i.e., time [h], pressure [*P*], temperature [*T*]) of each raw material to achieve the maximum specific mechanical properties

Material	Specific mechanical properties (J/g)	Maximum values	h	*P* (MPa)	*T* (°C)
S	σ_U/ρ	7.42	16	6.75	90
	E/ρ	2,481.9	16	6.75	90
	U_T/ρ	0.061	16	6.75	80
SM	σ_U/ρ	7.45	8	20.27	90
	E/ρ	2,521.3	16	20.27	90
	U_T/ρ	0.043	8	20.27	90
HCM	σ_U/ρ	10.32	4	20.27	100
	E/ρ	2,912.3	4	20.27	100
	U_T/ρ	0.034	16	6.75	90

predictors and the specific material properties (i.e., ρ, σ_U, E, U_T) as output responses of each mechanical sample and developed a neural network model as summarized in Figure 5. This model aims to map the output values from any given predictor values instead of running the specific experimental test.[65,66] Instead of directly predicting the mechanical properties, we use a k-means clustering method[67–70] to divide the N tests into five levels for each σ_U, E, and U_T (see the details of this clustering algorithm in the experimental procedures). Each sample is labeled by a 4-element vector $\vec{V}$, with each element V_i taking the response value from 0 to 4 for a specific material property. Hence, any samples with the same V_i value will have a similar corresponding material property compared with other samples. We build a tri-layered neural network model with a uniform layer size for each layer to find the correlation between the processing conditions and material property. Figure S4 shows the confusion matrix for each model. It is shown that for training and testing data, the predicted response value V_{i_pred} is largely aligned with the actual test result V_i for each material property, with over 70% of predictions being accurate or only one level different from the level of the test result, as $\left|V_{i\_pred} - V_i\right| \leq 1$.

We use the neuron network models to predict the optimal processing condition that yields the highest specific mechanical properties. We randomly generate 100,000 sets of feasible processing conditions, as shown by points in Figure 6, and use the models to predict ρ and mechanical properties and further compute σ_U/ρ, E/ρ, and U_T/ρ values that correspond to each feasible condition (as plotted in Figure S5). Then, we normalize each dimension of the different processing conditions and cluster them together with the predicted specific mechanical properties by k-means (see the experimental procedures for details), which enables us to identify the cluster of processing conditions that yields the highest specific mechanical property. Figure 6 highlights the location of all the points within the cluster of the highest σ_U/ρ, E/ρ, and U_T/ρ values, suggesting the range of the most favorable processing conditions for a particular specific mechanical property.

We summarize the range of the data points of the last cluster by computing the mean values and the deviation for the processing conditions and the specific mechanical properties (Table S4). These predictions agree with the tensile test observations (Table 2), as shown in Figure S6. Furthermore, it is shown that the machine learning models predict some specific mechanical properties to be higher than the direct experimental observation, and the corresponding processing conditions agree with the tensile tests. The learning model predicts according to the trend of all the testing results, while the direct observation is obtained from a single sample test that may be subjected to many random factors.

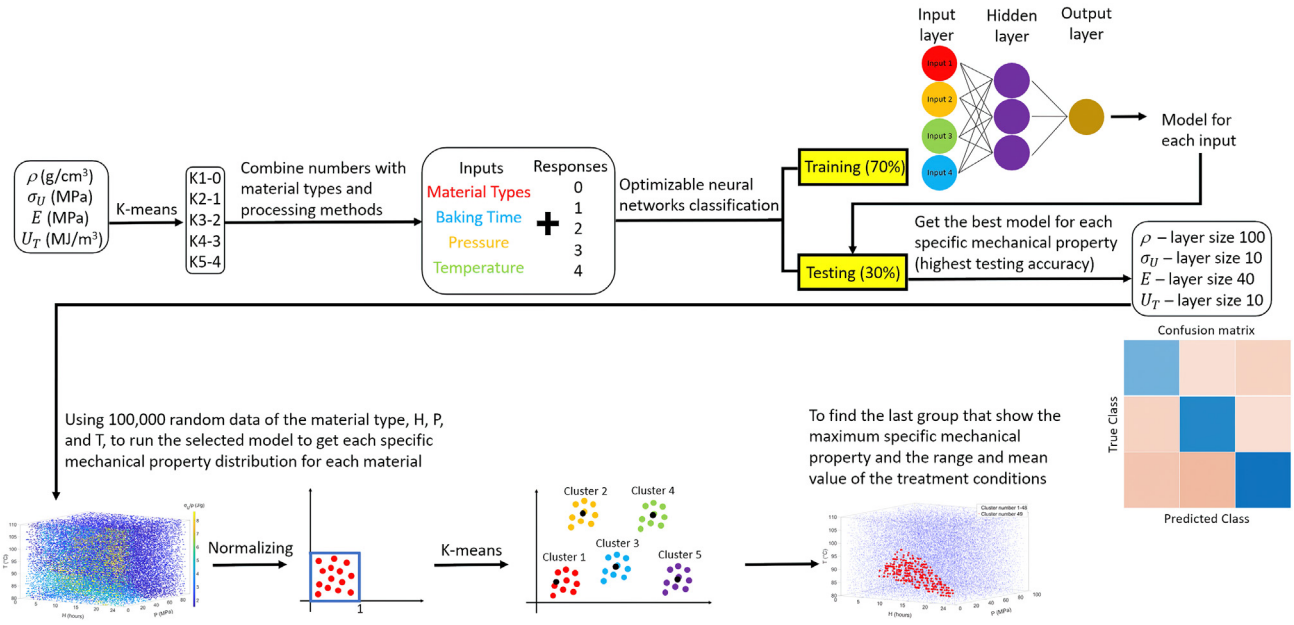

Figure 5. The general process of data clustering and the tri-layered neural network classification method for making predictions beyond experimental tests

The mycelium-based biocomposite as an environmentally friendly material shows more advantages in many applications (e.g., packaging materials, acoustic and thermal insulation boards) and is receiving more attention.[55,71] However, the development of biocomposite materials is still in its infancy, and the standardized procedure that will result in optimum material properties has yet to be discovered. Therefore, a novel manufacturing method for producing mycelium-based biocomposite samples is developed in the current article. Compared with literature methods that directly inoculated mycelium in the substrate for manufacturing samples,[43,44,72] we use the blender to mix the mycelium with wood fibers and water before heat pressing the composite that may enable us to further dissolve chitin and enable it to become exposed and get more distributed to interact with cellulose fibers at their interfaces, which leads to reinforcement and strength.[72] Because of the promising applications[73–76] and intrinsic environmentally friendly features over materials that require the heavy involvement of synthetic chemistry, the development of mycelium-based wood composites will need to start in the lab to fully understand the mechanisms of the mycelium growth and the structure-mechanics relationship at the microscopic scale in our fundamental studies but will eventually aim to scale up to large-scale manufacturing for engineering applications including infrastructure and packaging. Indeed, its structural designs and applications in buildings for thermal insulation, fire resistance, and acoustic absorption will be further explored, and complex structures and their related material functions will be evaluated,[77] for example, via 3D printing and foam forming. However, it is crucial to identify a sustainable way that requires less energy consumption and carbon emission but yields materials of higher specific mechanics during manufacturing.[78] This will give the large-scale manufacturing of the material commercial advantages over other conventional building and packaging materials. Compared with traditional engineering materials such as polymer matrix composites, mycelium-based wood composites have many limitations (e.g., shaping, time cost), motivating us to work with industrial units to understand the critical challenge in making the breakthrough that will lead to its mass production.

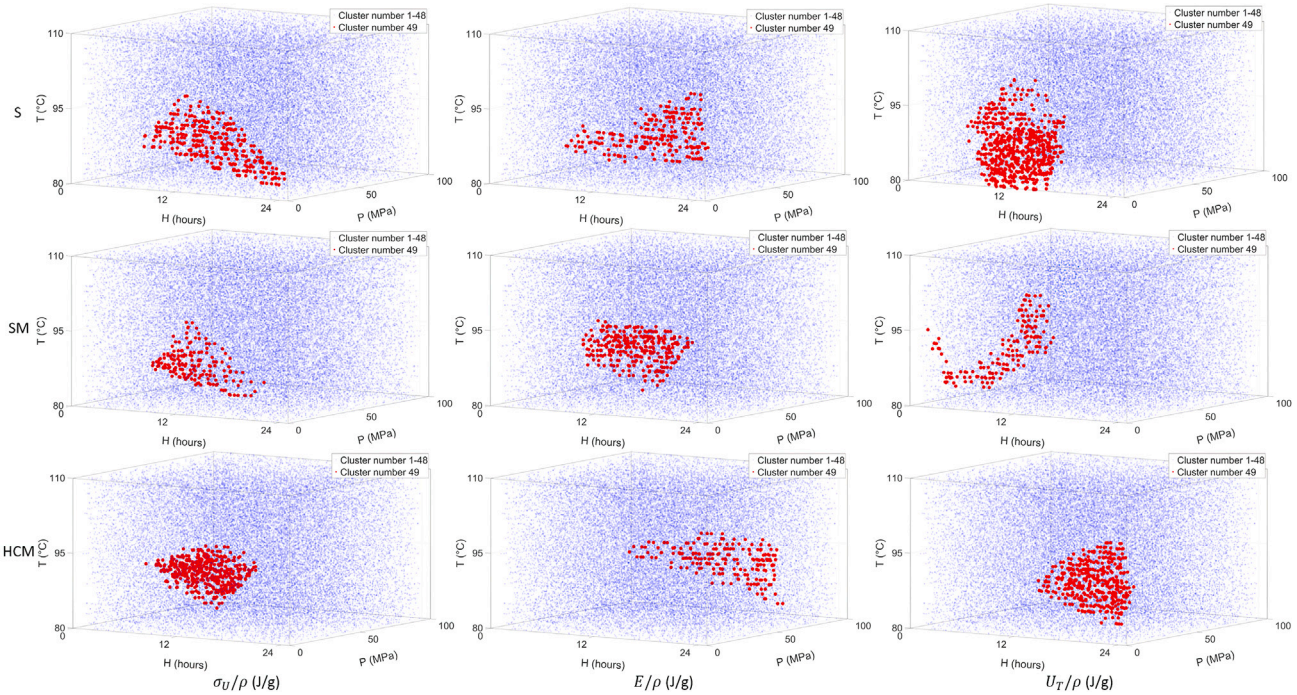

Figure 6. 3D scatterplots for the processing conditions of randomly generated 100,000 imaginary samples made of different raw materials (stalk [S], stalk with mycelium [SM], and hardwood mixed with coffee grounds and mycelium [HCM]), with the points corresponding to the highest specific mechanical properties (σ_U/ρ, E/ρ, and U_T/ρ) highlighted by a red color

Conclusions

Our results show that adding the mycelium to the wood composite will be promising for specific strength and *E*. It requires higher pressure but less baking time to achieve optimal mechanics. Our machine learning results point out that a pressure 2–3 times (for SM and HCM samples) that of the highest pressure for current experimental tests can be beneficial. The temperature requirement is similar for all wood composites, with and without mycelium, around 90°C. Optimizing the toughness of samples with mycelium seems more complicated, and a long baking time and low pressure are essential. Comparing the machine learning results with the experiment results, the general trends of the effect of baking time, pressure, and temperature on sample mechanics are the same.

The mycelium species and substrate type we chose for this study are commonly accessible for repeating tests. Integrating experimental tests with machine learning has opened up a new frontier for predicting multiphysics phenomena within high-dimensional design spaces that would be difficult to explore through traditional experimentation alone. Our experiment showed that by integrating experimental tests with machine learning, we could obtain multiphysics predictions within a high-dimensional design space that the experiment tests cannot immediately fully explore. By training these algorithms on a wide range of experimental data, we were able to create predictive models that could explore complex relationships between various factors in the design space, enabling us to generate more accurate predictions about how these factors interact with one another. The predictions can help design conditions for further improvement. Our model can guide future experimental synthesis and characterization and be updated by having more upcoming test results, making the prediction more accurate. We plan to increase the

dimension of our study beyond the processing conditions summarized in the current article and include the growth of mycelium. The effects of incubation temperature, humidity, nutrients supplied, and light need to be quantitatively understood. Moreover, the mycelium species and substrate type will lead to many possibilities and will be investigated in our incoming work.

EXPERIMENTAL PROCEDURES

Resource availability

Lead contact

Further information and requests for resources and reagents should be directed to and will be fulfilled by the lead contact, Zhao Qin (zqin02@syr.edu).

Materials availability

Composites generated in this study will be made available on request, but we may require a payment and/or a completed materials transfer agreement if there is potential for commercial application.

Data and code availability

All experimental data is included in the supplementary information available online. Other requests for the research details will be made by contacting the lead contact.

General information on the experiment

The general process of our experiment is that we grow the mycelium of *P. eryngii* on S particles and fibers. We use a heat press to turn the mixture of the mycelium and growing medium into mechanical samples in different processing conditions and characterize their mechanical functions. We use machine learning, enabled by an artificial neural network, to build a model based on the experimental data that predicts the key mechanical features of the composite for different treatment conditions.

Preparation of mechanical samples

We first culture the spore on agar substrate for 7 days before cutting them into small pieces and mixing them with the grains in jars for another 7 days until the white fibers occupy most of the space in the jar. We then migrate the grains with the mycelium to the culture bag filled with the S substrate (weight ratio 1:5; Figure S1B). We keep the culture bag at room temperature (around 25°C) and use the ultrasonic humidifier to generate water mist to keep the growth environment at high humidity (relatively 98%) for 14 days (SM). For control, we prepare a substrate material by mixing pure Ss with wet gains with the same weight ratio (5:1) and allow them to rest in the growing environment for 7 days to obtain the combination without mycelium fibers (S). For the HCM, we also culture the kit for 7 days in the same high humidity condition.

To ascertain whether mycelium can or cannot improve the material's mechanical properties, we prepare three different materials for the tensile test: S, SM, and HCM. Figure S1B shows the three different materials. We use these three different raw materials for mechanical tests. We take ~200 g raw materials each time into a blender, add 200 g water, and blend the mixture until it becomes mushy. Next, we place a portion of the mixture in an aluminum dog bone-shaped mold and compress the upper layer of the mold against the bottom layer by using a 10-ton heat-press machine with the hydraulic hand pump, as shown in Figure 2A, to perform the heat press and make the dog bone samples. The remaining mixture is stored in a sterilized plastic box in the refrigerator to keep it at a lower temperature before the heat press.

Mold design

We design a two-part mold to make the mycelium-based biocomposite sample of a type IV dog bone-shape according to the ASTM D638 standard. The sample has a shoulder at each end and a gauge section, which causes a stress concentration to occur in the middle when the sample is loaded with a tensile force. Figure S1A shows the aluminum mold, including the top and bottom parts, which are all aluminum. For the top part, the length of the dog bone shape is 114 mm, the width at the two ends is 18 mm, and the width of the narrow part in the middle is 5 mm. The effective pressure area of the top part is 1,370.11 mm^2. We design the corners and the connecting parts into a curved transition because of the mechanical requirements. To make it easy to remove the upper part after heat press, the length and width of the bottom groove part are all longer than the top part, about 1.7 mm. We polish the side of the top of the dog bone-shaped mold about 1° from top to bottom. We also open four holes at the bottom part and make an aluminum plate that could be put into the bottom part. To prevent the mycelium-based material adhesive from sticking to the top part of the aluminum plate after the high-temperature baking, we cut aluminum foil in the dog bone shape and place it inside the mold before placing the materials.

Heat-press procedure

The press machine connected with the proportional-integral-derivative (PID) temperature controller box allows us to set different temperatures (Figure 2A). We select three different temperatures for each material (i.e., 80°C, 90°C, and 100°C) and three different applied press forces, which are 1, 2, and 3 metric tons. We convert the applied force to the pressure on the sample with

$$\sigma_{press} = \frac{F_{plate}}{A} \quad \text{(Equation 1)}$$

where σ_{press} and F_{plate} are the normal stress and force applied on the top surface of the sample, respectively, and A = 13.68 cm^2 is the area of top surface of the dog-bone sample. The three applied pressures lead to pressures of 6.75, 13.51, and 20.27 MPa, respectively. For each sample, we set the targeting temperature first. When the temperature reaches the one designated, we put the mold with the material on the bottom plate of the machine and begin to apply the pressure. We use the paper towel to wipe off excess water squeezed out after applying the target load. We allow the machine to bake the sample until the time that we are setting and then take the mold off the machine. Usually, the press machine will drop the pressure automatically, so we need to apply pressure so that the machine will stay at the aim load that we set. For each material (i.e., S, SM, and HCM), we have three different temperatures combined with three different pressures for each material. We set the five baking times for each combination: 1, 2, 4, 8, and 16 h. We have prepared 45 samples for each material for mechanical tests.

Tensile test and density measurement

We perform the tensile tests on each dog bone sample with an Instron 5966 machine (10 kN static load cell, 1 kN pneumatic grips with 90 psi [0.62 MPa] holding pressure) to obtain its stress-strain curves in tension. We measure the initial sample length as the distance between the edges of the two grips as L_0 before the test. The lower grips are fixed, and the upper grips move at a constant displacement speed of v = 0.5 mm/min during our tests. The traveling distance of the upper grips is given by d at any time after the test starts, updated every 0.02 s, and the engineering strain of the sample is defined by $\varepsilon = \frac{d}{L_0}$. The load cell records the loading force f and computes the engineering stress with $\sigma = \frac{f}{A_0}$, where A_0 is the initial middle part cross-section area of the testing region of the dog bone sample. The test automatically

stops when the sample is broken. We use the $\varepsilon - \sigma$ data from $\varepsilon = 0$ to $\varepsilon = 0.001$ to perform the linear fitting and measure the slope of the fitting curve to calculate E. We measure the maximum stress of the entire $\varepsilon - \sigma$ curve as the ultimate stress. We measure the area under the entire stress-strain curve to obtain the toughness modulus. We measure the total weight of the sample m and use the equation $\rho = \frac{m}{A\bar{t}}$ to calculate the sample density, where A is the area of each sample and $\bar{t}$ is the average sample thickness, which is taken by a micrometer several times at different places for the average.

K-means clustering before machine learning

Due to the limited number of tests (n = 135) and randomness in the experiment, we could not directly predict the numeric values of all the specific mechanical properties with a high accuracy. We categorize the test samples for each of their material properties (i.e., ρ, σ_U, E, U_T) into five levels (scale 0–4) by using K-means.[67–70] K-means clustering is an algorithm to cluster objects based on certain attributes into a predetermined number (k) of clusters. The grouping is done by minimizing the sum of squares of distances between individual data and the corresponding cluster center, calculated by averaging all data within the cluster. It is an iterative procedure that refines the groupings in multiple steps, each improving the cluster quality.[79] We use the squared Euclidean distances to calculate the distance between each data point to the cluster center. Moreover, since the number of our experiment results is only 135, to avoid uneven grouping, we set a minimum of 25 data in a group, allowing each group to have the similar amount of data. We build a tri-layered neural network model with a uniform layer size for each layer, as the number of hidden neurons, to find the correlation between the processing conditions and a material property. Using 70% for training and 30% for testing, we adjust the layer size from 10 to 100 to obtain a highest testing accuracy without significantly overfitting. We end up with layer sizes of 100, 10, 40, and 10 for models in predicting ρ, σ_U, E, and U_T, respectively.

K-means clustering for scanning the promising processing conditions

After massively predicting and computing the σ_U/ρ, E/ρ, and U_T/ρ values for the 100,000 sets of feasible processing conditions, we normalize the processing conditions and the predicted specific mechanical properties by computing the standardizing values (Z scores) for each dimension and use them to categorize the different processing conditions and a specific mechanical property (for same skewness and kurtosis[80–82]). We increase the number of clusters (k) to determine when the mean value of the cluster that corresponds to the highest specific mechanical property converges to a constant level. It is shown in Figure S7 that $k = 49$ yields the convergence for all specific mechanical properties for different raw materials. We use $k = 49$ to filter out the cluster of the highest specific mechanics values and highlight these data points in Figure 6.

SUPPLEMENTAL INFORMATION

Supplemental information can be found online at https://doi.org/10.1016/j.xcrp.2023.101424.

ACKNOWLEDGMENTS

The authors acknowledge Tim Breen's help with the design and manufacture of the dog bone mold and valuable discussion with Dr. Eric Finkelstein and Dr. Debra Driscoll for microscopic characterization of mycelium fibers. The authors acknowledge the National Science Foundation CAREER Grant (CMMI-2145392) and Collaboration

for Unprecedented Success and Excellence (CUSE) Grants at Syracuse University for supporting the research work.

AUTHOR CONTRIBUTIONS

Z.Q. proposed, designed, and supervised the research. L.Y. prepared the composite samples, performed the mechanical tests, and took the microscopic images. L.Y. and Z.Q. analyzed the mechanical test results and microscopic characterizations. L.Y. and Z.Q. built the machine learning models and performed the prediction. Z.Q. and L.Y. wrote the manuscript and revised and approved the manuscript.

DECLARATION OF INTERESTS

The authors declare no competing interests.

Received: March 13, 2023
Revised: April 24, 2023
Accepted: May 2, 2023
Published: May 24, 2023

REFERENCES

1. Pizzi, A., Papadopoulos, A.N., and Policardi, F. (2020). Wood composites and their polymer binders. Polymers *12*, 1115. https://doi.org/10.3390/POLYM12051115.

2. Gardner, D.J., Han, Y., and Wang, L. (2015). Wood–Plastic composite technology. Curr. For. Rep. *1*, 139–150. https://doi.org/10.1007/s40725-015-0016-6.

3. Mazzanti, V., and Mollica, F. (2020). A review of wood polymer composites rheology and its implications for processing. Polymers *12*, 2304. https://doi.org/10.3390/polym12102304.

4. Schneider, M.H. (1994). Wood-polymer composites - society of wood science and technology state-of-the-art review paper. Wood Fiber Sci. *26*, 142–151.

5. Bazli, M., Heitzmann, M., and Villacorta Hernandez, B. (2022). Durability of fibre-reinforced polymer-wood composite members: an overview. Compos. Struct. *295*, 115827. https://doi.org/10.1016/J.COMPSTRUCT.2022.115827.

6. Oksman, K. (1996). Improved interaction between wood and synthetic polymers in wood/polymer composites. Wood Sci. Technol. *30*, 179–205. https://doi.org/10.1007/BF00231633.

7. Krišťák, L., and Réh, R. (2021). Application of wood composites. Appl. Sci. *11*, 2479. https://doi.org/10.3390/app11083479.

8. Adekomaya, O., Jamiru, T., Sadiku, R., and Huan, Z. (2016). A review on the sustainability of natural fiber in matrix reinforcement – a practical perspective. J. Reinforc. Plast. Compos. *35*, 3–7. https://doi.org/10.1177/0731684415611974.

9. Kumar, V., Tyagi, L., and Sinha, S. (2011). Wood flour-reinforced plastic composites: a review. Rev. Chem. Eng. *27*, 253–264. https://doi.org/10.1515/REVCE.2011.006.

10. Kokta, B.v., Chen, R., Daneault, C., and Valade, J.L. (1983). Use of wood fibers in thermoplastic composites. Polym. Compos. *4*, 229–232. https://doi.org/10.1002/pc.750040407.

11. Ormondroyd, G.A. (2015). Adhesives for wood composites. Wood Composites, 47–66. https://doi.org/10.1016/B978-1-78242-454-3.00003-2.

12. Papadopoulos, A.N. (2019). Advances in wood composites. Polymers *12*, 48. https://doi.org/10.3390/polym12010048.

13. Papadopoulos, A.N. (2020). Advances in wood composites II. Polymers *12*, 1552. https://doi.org/10.3390/polym12071552.

14. Bharath, K.N., and Basavarajappa, S. (2016). Applications of biocomposite materials based on natural fibers from renewable resources: a review. Sci. Eng. Compos. Mater. *23*, 123–133. https://doi.org/10.1515/secm-2014-0088.

15. Jin, K., Qin, Z., and Buehler, M.J. (2015). Molecular deformation mechanisms of the wood cell wall material. J. Mech. Behav. Biomed. Mater. *42*, 198–206. https://doi.org/10.1016/j.jmbbm.2014.11.010.

16. Sun, Y., Guo, L., Liu, Y., Wang, W., and Song, Y. (2019). Glue wood veneer to wood-fiber–high-density-polyethylene composite. Int. J. Adhesion Adhes. *95*, 102444. https://doi.org/10.1016/j.ijadhadh.2019.102444.

17. Ye, H., Wang, Y., Yu, Q., Ge, S., Fan, W., Zhang, M., Huang, Z., Manzo, M., Cai, L., Wang, L., and Xia, C. (2022). Bio-based composites fabricated from wood fibers through self-bonding technology. Chemosphere *287*, 132436. https://doi.org/10.1016/j.chemosphere.2021.132436.

18. Xu, C., Sun, C., Wan, H., Tan, H., Zhao, J., and Zhang, Y. (2022). Microstructure and physical properties of poly(lactic acid)/polycaprolactone/rice straw lightweight bio-composite foams for wall insulation. Construct. Build. Mater. *354*, 129216. https://doi.org/10.1016/j.conbuildmat.2022.129216.

19. Zhang, B., Zheng, B., Wang, X., Shi, Q., Jia, J., Huo, Y., Pan, C., Han, J., and Chen, M. (2017). Improvement of the water resistance of soybean protein-based wood adhesive by a thermo-chemical treatment approach. Int. J. Adhesion Adhes. *17*, 222–226. https://doi.org/10.1016/j.ijadhadh.2017.08.002.

20. Kumar, C., and Leggate, W. (2022). An overview of bio-adhesives for engineered wood products. Int. J. Adhesion Adhes. *118*, 103187. https://doi.org/10.1016/J.IJADHADH.2022.103187.

21. Jiang, W., Kumar, A., and Adamopoulos, S. (2018). Liquefaction of lignocellulosic materials and its applications in wood adhesives—a review. Ind. Crop. Prod. *124*, 325–342. https://doi.org/10.1016/j.indcrop.2018.07.053.

22. Kaseem, M., Hamad, K., Deri, F., and Ko, Y.G. (2015). Material properties of polyethylene/wood composites: a review of recent works. Polym. Sci. *57*, 689–703. https://doi.org/10.1134/S0965545X15070068.

23. Hüttermann, A., Mai, C., and Kharazipour, A. (2001). Modification of lignin for the production of new compounded materials. Appl. Microbiol. Biotechnol. *55*, 387–394. https://doi.org/10.1007/s002530000590.

24. Youngquist, J.A. (1999). Wood-based composites and panel products. In Wood handbook : wood as an engineering material, pp. 10.1–10.31.

25. Ferdosian, F., Pan, Z., Gao, G., and Zhao, B. (2017). Bio-based adhesives and evaluation for wood composites application. Polymers *9*, 70. https://doi.org/10.3390/polym9020070.

26. Hemmilä, V., Adamopoulos, S., Karlsson, O., and Kumar, A. (2017). Development of sustainable bio-adhesives for engineered wood panels-A Review. RSC Adv. *7*, 38604–38630. https://doi.org/10.1039/c7ra06598a.

27. Kadla, J.F., Kubo, S., Venditti, R.A., Gilbert, R.D., Compere, A.L., and Griffith, W. (2002). Lignin-based carbon fibers for composite fiber

applications. Carbon N. Y. *40*, 2913–2920. https://doi.org/10.1016/S0008-6223(02)00248-8.

28. Irvine, G.M. (1985). The significance of the glass transition of lignin in thermomechanical pulping. Wood Sci. Technol. *19*, 139–149. https://doi.org/10.1007/BF00353074.

29. Vázquez, G., González, J., Freire, S., and Antorrena, G. (1997). Effect of chemical modification of lignin on the gluebond performance of lignin-phenolic resins. Bioresour. Technol. *60*, 191–198. https://doi.org/10.1016/S0960-8524(97)00030-8.

30. Din, Z., Chen, L., Xiong, H., Wang, Z., Ullah, I., Lei, W., Shi, D., Alam, M., Ullah, H., and Khan, S.A. (2020). Starch: an undisputed potential candidate and sustainable resource for the development of wood adhesive. Starch/Staerke *72*, 1900276. https://doi.org/10.1002/star.201900276.

31. Tan, H., Zhang, Y., and Weng, X. (2011). Preparation of the plywood using starch-based adhesives modified with blocked isocyanates. Procedia Eng. *15*, 1171–1175. https://doi.org/10.1016/j.proeng.2011.08.216.

32. Onusseit, H. (1992). Starch in industrial adhesives: new developments. Ind. Crop. Prod. *1*, 141–146. https://doi.org/10.1016/0926-6690(92)90012-K.

33. Jumper, J., Evans, R., Pritzel, A., Green, T., Figurnov, M., Ronneberger, O., Tunyasuvunakool, K., Bates, R., Žídek, A., Potapenko, A., et al. (2021). Highly accurate protein structure prediction with AlphaFold. Nature *596*, 583–589. https://doi.org/10.1038/s41586-021-03819-2.

34. Li, N., Qi, G., Sun, X.S., Stamm, M.J., and Wang, D. (2012). Physicochemical properties and adhesion performance of canola protein modified with sodium bisulfite. J. Americ. Oil Chem. Soc. *89*, 897–908. https://doi.org/10.1007/s11746-011-1977-7.

35. Pérez, S., and Bertoft, E. (2010). The molecular structures of starch components and their contribution to the architecture of starch granules: a comprehensive review. Starch/Staerke *62*, 389–420. https://doi.org/10.1002/star.201000013.

36. Sun, W., Tajvidi, M., Howell, C., and Hunt, C.G. (2020). Functionality of surface mycelium interfaces in wood bonding. ACS Appl. Mater. Interfaces *12*, 57431–57440. https://doi.org/10.1021/acsami.0c18165.

37. Sun, W., Tajvidi, M., Hunt, C.G., McIntyre, G., and Gardner, D.J. (2019). Fully bio-based hybrid composites made of wood, fungal mycelium and cellulose nanofibrils. Sci. Rep. *9*, 3766. https://doi.org/10.1038/s41598-019-40442-8.

38. Saez, D., Grizmann, D., Trautz, M., and Werner, A. (2022). Exploring the binding capacity of mycelium and wood-based composites for use in construction. Biomimetics *7*, 78. https://doi.org/10.3390/biomimetics7020078.

39. Attias, N., Danai, O., Abitbol, T., Tarazi, E., Ezov, N., Pereman, I., and Grobman, Y.J. (2020). Mycelium bio-composites in industrial design and architecture: comparative review and experimental analysis. J. Clean. Prod. *246*, 119037. https://doi.org/10.1016/j.jclepro.2019.119037.

40. Abdelhady, O., Spyridonos, E., and Dahy, H. (2023). Bio-modules: mycelium-based composites forming a modular interlocking system through a computational design towards sustainable architecture. Design *7*, e10020. https://doi.org/10.3390/designs7010020.

41. Yang, L., Park, D., and Qin, Z. (2021). Material function of mycelium-based bio-composite: a review. Front. Mater. *8*, 1–17. https://doi.org/10.3389/fmats.2021.737377.

42. Sivaprasad, S., Byju, S.K., Prajith, C., Shaju, J., and Rejeesh, C.R. (2021). Development of a novel mycelium bio-composite material to substitute for polystyrene in packaging applications. Mater. Today: Proc. *47*, 5038–5044. https://doi.org/10.1016/j.matpr.2021.04.622.

43. Jiang, L., Walczyk, D., McIntyre, G., Bucinell, R., and Tudryn, G. (2017). Manufacturing of biocomposite sandwich structures using mycelium-bound cores and preforms. J. Manuf. Process. *28*, 50–59. https://doi.org/10.1016/j.jmapro.2017.04.029.

44. Appels, F.V., Camere, S., Montalti, M., Karana, E., Jansen, K.M., Dijksterhuis, J., Krijgsheld, P., and Wösten, H.A. (2019). Fabrication factors influencing mechanical, moisture- and water-related properties of mycelium-based composites. Mater. Des. *161*, 64–71. https://doi.org/10.1016/j.matdes.2018.11.027.

45. Jones, M., Mautner, A., Luenco, S., Bismarck, A., and John, S. (2020). Engineered mycelium composite construction materials from fungal biorefineries: a critical review. Mater. Des. *187*, 108397. https://doi.org/10.1016/j.matdes.2019.108397.

46. Haneef, M., Ceseracciu, L., Canale, C., Bayer, I.S., Heredia-Guerrero, J.A., and Athanassiou, A. (2017). Advanced materials from fungal mycelium: fabrication and tuning of physical properties. Sci. Rep. *7*, 41292. https://doi.org/10.1038/srep41292.

47. Jiang, L., Zheng, A., Zhao, Z., He, F., Li, H., and Wu, N. (2016). Cost modeling and optimization of a manufacturing system for mycelium-based biocomposite parts. J. Manuf. Syst. *200*, 8–13. https://doi.org/10.1016/j.jmsy.2016.07.004.

48. Sydor, M., Bonenberg, A., Doczekalska, B., and Cofta, G. (2021). Mycelium-based composites in art, architecture, and interior design: a review. Polymers *14*, 145. https://doi.org/10.3390/polym14010145.

49. Girometta, C., Picco, A.M., Baiguera, R.M., Dondi, D., Babbini, S., Cartabia, M., Pellegrini, M., and Savino, E. (2019). Physico-mechanical and thermodynamic properties of mycelium-based biocomposites: a review. Sustainability *11*, 281. https://doi.org/10.3390/su11010281.

50. Jose, J., Uvais, K.N., Sreenadh, T.S., Deepak, A.v., and Rejeesh, C.R. (2021). Investigations into the development of a mycelium biocomposite to substitute polystyrene in packaging applications. Arabian J. Sci. Eng. *46*, 2975–2984. https://doi.org/10.1007/s13369-020-05247-2.

51. Pelletier, M.G., Holt, G.A., Wanjura, J.D., Bayer, E., and McIntyre, G. (2013). An evaluation study of mycelium based acoustic absorbers grown on agricultural by-product substrates. Ind. Crop. Prod. *51*, 480–485. https://doi.org/10.1016/j.indcrop.2013.09.008.

52. Jones, M., Bhat, T., Huynh, T., Kandare, E., Yuen, R., Wang, C.H., and John, S. (2018). Waste-derived low-cost mycelium composite construction materials with improved fire safety. Fire Mater. *42*, 816–825. https://doi.org/10.1002/fam.2637.

53. Dias, P.P., Jayasinghe, L.B., and Waldmann, D. (2021). Investigation of Mycelium-Miscanthus composites as building insulation material. Results in Materials *10*, 100189. https://doi.org/10.1016/j.rinma.2021.100189.

54. Gonzalez, P., and Labarère, J. (2000). Phylogenetic relationships of Pleurotus species according to the sequence and secondary structure of the mitochondrial small-subunit rRNA V4, V6 and V9 domains the GenBank accession numbers for the sequences reported in this paper are given in Methods. Microbiology (N. Y.) *146*, 209–221. https://doi.org/10.1099/00221287-146-1-209.

55. Sydor, M., Cofta, G., Doczekalska, B., and Bonenberg, A. (2022). Fungi in mycelium-based composites: usage and recommendations. Materials *15*, 6283. https://doi.org/10.3390/ma15186283.

56. Gautam, A.K., Verma, R.K., Avasthi, S., Bohra, Y., Devadatha, B., Niranjan, M., and Suwannarach, N. (2022). Current insight into traditional and modern methods in fungal diversity estimates. J. Fungi *8*, 226. https://doi.org/10.3390/jof8030226.

57. Tong, J., Gao, H., Weng, Y., and Wang, Y. (2022). Anisotropic aerogels with excellent mechanical resilience and thermal insulation from Pleurotus eryngii fungus. Macromol. Mater. Eng. *308*, 2200538. https://doi.org/10.1002/mame.202200538.

58. Back to the Roots (America's Organic Gardening Company) https://backtotheroots.com/?gclid=CjwKCAiAnZCdBhBmEiwA8nDQxUPWX7l-Pxv41bRByR98Iw9VqyEDdwnUFkjhJg7XC19MD1I_t31ORBoCi1gQAvD_BwE.

59. Wu, T., Wang, X., and Kito, K. (2015). Effects of pressures on the mechanical properties of corn straw bio-board. Engineering in Agriculture, Environment and Food *8*, 123–129. https://doi.org/10.1016/j.eaef.2015.07.003.

60. Gibson, L.J., and Ashby, M.F. (1997). Cellular Solids: Structure and Properties.

61. Santos, I.S., Nascimento, B.L., Marino, R.H., Sussuchi, E.M., Matos, M.P., and Griza, S. (2021). Influence of drying heat treatments on the mechanical behavior and physico-chemical properties of mycelial biocomposite. Compos. B Eng. *217*, 108870. https://doi.org/10.1016/j.compositesb.2021.108870.

62. Wegst, U.G.K., Bai, H., Saiz, E., Tomsia, A.P., and Ritchie, R.O. (2015). Bioinspired structural materials. Nat. Mater. *14*, 23–36. https://doi.org/10.1038/nmat4089.

63. Martínez-Hergueta, F., Ridruejo, A., González, C., and Llorca, J. (2015). Deformation and energy dissipation mechanisms of needle-punched nonwoven fabrics: a multiscale experimental analysis. Int. J. Solids Struct.

64-65, 120–131. https://doi.org/10.1016/j.ijsolstr.2015.03.018.

64. Picu, C.R. (2021). Constitutive models for random fiber network materials: a review of current status and challenges. Mech. Res. Commun. *114*, 103605. https://doi.org/10.1016/j.mechrescom.2020.103605.

65. Baughman, D.R., and Liu, Y.A. (1995). Classification: fault diagnosis and feature categorization. In Neural Networks in Bioprocessing and Chemical Engineering, pp. 110–171. https://doi.org/10.1016/b978-0-12-083030-5.50009-6.

66. Izadkhah, H. (2022). Classification in bioinformatics. In Deep Learning in Bioinformatics (Elsevier), pp. 113–130. https://doi.org/10.1016/b978-0-12-823822-6.00013-5.

67. Arthur, D., and Vassilvitskii, S. (2007). K-means++: the advantages of careful seeding. In Proceedings of the Annual ACM-SIAM Symposium on Discrete Algorithms, pp. 1027–1035.

68. Lloyd, S. (1982). Least squares quantization in PCM. IEEE Trans. Inf. Theor. *28*, 129–137. https://doi.org/10.1109/TIT.1982.1056489.

69. Cooper, M., and Seber, G.A.F. (1985). Multivariate observations. J. Market. Res. *22*, 226. https://doi.org/10.2307/3151376.

70. Everitt, B., and Spath, H. (1985). Cluster dissection and analysis: theory, fortran programs and examples. J R Stat Soc Ser A *148*, 285. https://doi.org/10.2307/2981981.

71. Angelova, G.V., Brazkova, M.S., and Krastanov, A.I. (2021). Renewable mycelium based composite - sustainable approach for lignocellulose waste recovery and alternative to synthetic materials - a review. Z. Naturforsch., C: J. Biosci. *76*, 431–442. https://doi.org/10.1515/znc-2021-0040.

72. Karana, E., Blauwhoff, D., Hultink, E.J., and Camere, S. (2018). When the material grows: a case study on designing (with) mycelium-based materials. Int. J. Des. *12*, 119–136.

73. Li, L., Liang, T., Liu, W., Liu, Y., and Ma, F. (2020). A comprehensive review of the mycelial pellet: research status, applications, and future prospects. Ind. Eng. Chem. Res. *59*, 16911–16922. https://doi.org/10.1021/acs.iecr.0c01325.

74. Dhillon, G.S., Kaur, S., Brar, S.K., and Verma, M. (2013). Green synthesis approach: extraction of chitosan from fungus mycelia. Crit. Rev. Biotechnol. *33*, 379–403. https://doi.org/10.3109/07388551.2012.717217.

75. Vandelook, S., Elsacker, E., van Wylick, A., de Laet, L., and Peeters, E. (2021). Current state and future prospects of pure mycelium materials. Fungal Biol. Biotechnol. *8*, 20. https://doi.org/10.1186/s40694-021-00128-1.

76. Elsacker, E., Vandelook, S., van Wylick, A., Ruytinx, J., de Laet, L., and Peeters, E. (2020). A comprehensive framework for the production of mycelium-based lignocellulosic composites. Sci. Total Environ. *725*, 138431. https://doi.org/10.1016/j.scitotenv.2020.138431.

77. Gauvin, F., Tsao, V., Vette, J., and Brouwers, H.J.H. (2022). Physical properties and hygrothermal behavior of mycelium-based composites as foam-like wall insulation material. In Bio-Based Building Materials Construction Technologies and Architecture (Trans Tech Publications Ltd), pp. 643–651. https://doi.org/10.4028/www.scientific.net/CTA.1.643.

78. Ali, G., and Gürsoy, B. (2022). Challenges and advantages of building with mycelium-based composites: a review of growth factors that affect the material properties. In Fungal Biopolymers and Biocomposites: Prospects and Avenues, M. V., S.K.R. Deshmukh Sunil K. and Deshpande, eds. (Springer Nature Singapore), pp. 131–145. https://doi.org/10.1007/978-981-19-1000-5_8.

79. Sterling, T., Anderson, M., and Brodowicz, M. (2018). MapReduce. In High Performance Computing (Elsevier), pp. 579–589. https://doi.org/10.1016/b978-0-12-420158-3.00019-8.

80. Misra, S., Osogba, O., and Powers, M. (2019). Unsupervised outlier detection techniques for well logs and geophysical data. In Machine Learning for Subsurface Characterization (Elsevier), pp. 1–37. https://doi.org/10.1016/B978-0-12-817736-5.00001-6.

81. Molugaram, K., and Rao, G.S. (2017). Random variables. In Statistical Techniques for Transportation Engineering (Elsevier), pp. 113–279. https://doi.org/10.1016/B978-0-12-811555-8.00004-0.

82. Roessner, U., Nahid, A., Chapman, B., Hunter, A., and Bellgard, M. (2011). Metabolomics - the combination of analytical biochemistry, biology, and informatics. Comprehensive Biotechnology, 435–447. https://doi.org/10.1016/B978-0-444-64046-8.00027-6.